Self-assembly of thiolated versus non-thiolated peptide amphiphiles

Egorova, E.; Gooris, G.S.; Luther, P.; Bouwstra, J.A.; Kros, A.; Boyle, A.L.

Introducing the **CSBio II**

Automated Peptide Synthesizer

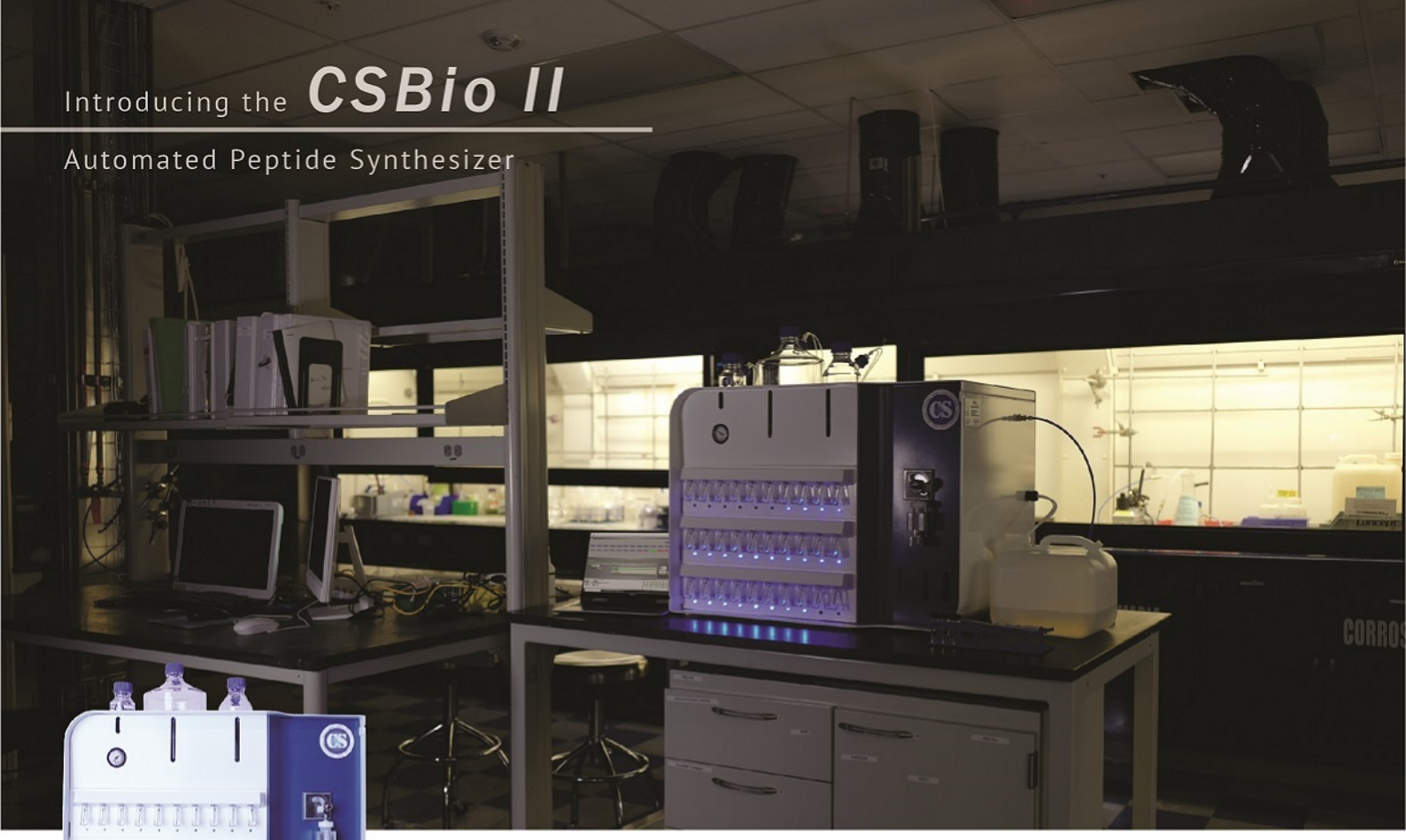

We will cover the night shift.

Easy to use

Make your 20 mer in < 5 hours

50 - 500mg of high purity peptide

CSBio INSTRUMENTATION

Whether you are tired of manual synthesis, waiting for ordered peptides or want to expand your lab's automated synthesis capabilities, the *CSBio II* is perfect for you. Set up your synthesis in minutes with just a few clicks and return to your finished peptide.

Your time is precious. Let the *CSBio II* maximize what you have.

See the *CSBio II* in action. Visit us at www.csbio.com/csbioii.html or contact us at instrument@csbio.com to schedule a virtual demo.

PEOPLE WHO LOVE PEPTIDES · PEOPLE WHO KNOW PEPTIDES

CSBIO INSTRUMENTATION | Peptide Synthesizers | DNA Synthesizers | Cleavage Systems | HPLC www.csbio.com | 650.525.6200

Received: 7 April 2021 | Revised: 23 June 2021 | Accepted: 28 June 2021

DOI: 10.1002/pep2.24236

ARTICLE

PeptideScience WILEY

Self-assembly of thiolated versus non-thiolated peptide amphiphiles

Elena A. Egorova[1] | Gert S. Gooris[2] | Prianka Luther[3] | Joke A. Bouwstra[2] | Alexander Kros[1] | Aimee L. Boyle[3]

[1]Supramolecular and Biomaterials Chemistry, Leiden Institute of Chemistry, Leiden University, Leiden, The Netherlands

[2]Division of BioTherapeutics, Leiden Academic Centre for Drug Research, Leiden University, Leiden, The Netherlands

[3]Macromolecular Biochemistry, Leiden Institute of Chemistry, Leiden University, Leiden, The Netherlands

Correspondence
Alexander Kros, Supramolecular and Biomaterials Chemistry, Leiden Institute of Chemistry, Leiden University, Leiden 2333 CC, The Netherlands.
Email: a.kros@chem.leidenuniv.nl

Aimee L. Boyle, Macromolecular Biochemistry, Leiden Institute of Chemistry, Leiden University, Leiden 2333 CC, The Netherlands.
Email: a.l.boyle@chem.leidenuniv.nl

Present address
Elena A. Egorova, Sirius University of Science and Technology, Sochi, Russia

Abstract

The self-assembly properties of peptide amphiphiles make them attractive for a range of applications, such as scaffolds for cell culture, drug delivery vehicles, or as stabilizing coatings for nanoparticles. The latter application requires derivatization of the amphiphiles to enable them to bind to, and interact with, a surface. This can be achieved by introduction of a thiol which facilitates binding to gold surfaces for example. However, small changes to the composition of peptide amphiphiles can have a large impact on their self-assembly behavior. Therefore, we have synthesized and characterized a range of amphiphiles with different peptide sequences, alkyl chain lengths, and with or without a terminal thiol. We have characterized their structure and self-assembly using circular dichroism (CD) spectroscopy, attenuated total reflection infrared (ATR-IR) spectroscopy, and transmission electron microscopy (TEM). We discuss how changes to the peptide sequence and alkyl chain affect self-assembly and compare the self-assembly properties of thiolated and non-thiolated amphiphiles. Such knowledge not only provides fundamental insights as to how self-assembly can be controlled, but will also be helpful in determining which amphiphiles are most suitable for use as stabilizing nanoparticle coatings.

KEYWORDS
peptide amphiphile, secondary structure, self-assembly

1 | INTRODUCTION

Gold nanoparticles (GNPs) have a wide range of applications in areas such as drug delivery,[1] photothermal therapy,[2,3] and sensing.[4–6] However, GNPs are typically synthesized with a citrate coating, which is unstable under physiological conditions. A different coating is therefore required in order for GNPs to be used for biological applications.[7,8] Polymers[9–11] or silica[12–14] are commonly used for this purpose. However, the effective size of the GNPs is often significantly increased due to the thickness of these coatings.[14] Therefore, low molecular weight molecules with stabilizing capabilities are of interest. It has been previously demonstrated that oligopeptides are able to stabilize small spherical GNPs (≤35 nm).[15,16] These peptides are tethered to a gold surface via a cysteine side chain resulting in covalent binding through Au—S bond formation.[17,18] The stabilizing effect of these peptides was partially attributed to their propensity to adopt β-structured self-assemblies both in solution and when attached to a gold surface.[19,20] However, these peptides also have limitations: their use for coating larger GNPs, or nonspherical GNPs, has not been reported.

To overcome the limitations of cysteine-containing peptides as GNP stabilizers, the use of peptide amphiphiles is proposed. Peptide amphiphiles are composed of a (polar) peptide segment conjugated to

an aliphatic chain.[21] Peptide amphiphiles are designed to form self-assembled supramolecular structures: in aqueous conditions a range of three-dimensional assemblies have been reported[21]; and two-dimensional assemblies are formed at interfaces.[22,23] If a thiol group is introduced at the terminus of the amphiphile's alkyl chain, it is possible to tether these molecules to a gold surface via an Au—S bond. In this arrangement, the gold core is surrounded with a hydrophobic environment created by the alkyl chains meaning the gold surface is shielded from undesired interactions with the biological medium. In addition, charged amino acids at the surface increase the colloidal stability of the GNPs due to increased repulsive forces.[17] Moreover, a high propensity to form β-sheets, which is typical for peptide amphiphiles, is an advantage for a GNP stabilizer.[24]

However, it is known that even small changes to the composition of a peptide amphiphile can affect the self-assembly properties.[24–27] Therefore any alterations made to either the alkyl chain (e.g., chain length, or inclusion of terminal functional groups such as thiols), or the amino acid sequence within the peptide domain need to be fully evaluated.

The aim of this study is to investigate how the self-assembly of different peptide amphiphiles changes when they are modified with thiols. For this, a thiol group was introduced at the alkyl chain terminus to yield functional peptide amphiphiles comprising valine (Val, V), alanine (Ala, A), and lysine (Lys, K) residues. Such amphiphiles are generally described as mercaptoacyl-$[VA]_3K_3$. Two different alkyl chains, 16-mercaptohexadecanoyl or 11-mercaptoundecanoyl were investigated as these are commonly employed in a variety of peptide amphiphiles.[21,28–30] For the peptide segment, inspiration was taken from the Stupp group and a $[VA]_3$ domain, representing four different peptide sequences: VVVAAA, AAAVVV, VAVAVA, and AVAVAV was studied. In addition, thiolated peptide amphiphiles were oxidized to form dimerized peptide amphiphiles with two alkyl chains and two identical peptide domains coupled via the formation of a disulfide bond. The effect of alkyl chain thiolation, alkyl chain length, and peptide composition on peptide amphiphile secondary structure was investigated using a variety of techniques. The propensities of non-thiolated and thiolated amphiphiles to form ordered secondary structures and to self-assemble into supramolecular fibers were evaluated with circular dichroism (CD) and attenuated total reflection infrared (ATR-IR) spectroscopy, as well as transmission electron microscopy (TEM). This approach not only allowed us to determine the effect of adding a thiol to the peptide amphiphile, but also enabled identification of peptide amphiphiles that exhibit peptide-driven self-assembly and are therefore candidates for GNP stabilization.

2 | MATERIALS AND METHODS

2.1 | Materials

All chemicals were purchased from Sigma-Aldrich except where stated otherwise. Fmoc-amino acids were obtained from Novabiochem. TFA, piperidine, DMF, DCM, methanol, and acetonitrile were purchased from Biosolve. Oxyma pure was supplied by Carl Roth GmbH. Formvar Carbon/Copper (200 mesh) TEM grids were purchased from Electron Microscopy Sciences.

2.2 | Peptide amphiphile synthesis

All peptide amphiphile sequences were synthesized by solid-phase peptide synthesis using standard Fmoc-chemistry protocols. The synthesis was performed on an automated microwave peptide synthesizer Liberty Blue (CEM). 20% piperidine in DMF was used as the deprotection agent and DIC/Oxyma were employed as activator/activator base. All sequences were synthesized on a Rink Amide resin. The alkyl chains were introduced via an on-resin coupling of the corresponding alkyl chain to the N-terminal amine of the corresponding peptide. The list of peptides and alkyl chains employed is shown in Scheme 1. All molecules were cleaved from the resin using a trifluoroacetic acid (TFA) cocktail with 1.5% deionized water, 2.5% triisopropylsilane (TIS), and 2.5% 3,4-ethylenedioxythiophene (EDOT) for thiolated peptide amphiphiles only. The crude amphiphiles were precipitated into cold diethyl ether, pelleted by centrifugation, redissolved in water, and lyophilized prior to purification.

2.3 | Peptide amphiphile purification

HPLC purification was performed on a Shimadzu system equipped with two LC-20AR pumps, an SPD-20A UV-Vis detector and a Phenomenex Kinetex EVO C18 column. The mobile phases were water and acetonitrile, containing 0.1% TFA. The purity of the compounds was assessed using LC-MS (Figures S1-S15). VariPure IPE (PL3540-D603VP, 100 mg, Agilent) columns were used to capture and remove TFA traces from the sample after purification and drying.

2.4 | Peptide amphiphile dimerization

Dimerization was conducted via oxidation of terminal thiols with iodine to form a disulfide bond. A peptide amphiphile was dissolved in 80% methanol at a concentration of 2 mg/mL and 0.5 M iodine solution was added dropwise to the stirred solution. The addition of iodine was stopped as soon as the color became persistently yellow. Stirring was continued for another 15 minutes and excess iodine was quenched with 1 M ascorbic acid. Methanol was evaporated and the presence of the dimers was confirmed with LC-MS. Dimerized amphiphiles were purified and lyophilized prior to analysis in the manner described above. The purity of the compounds was assessed using LC-MS (Figures S16-S25).

2.5 | CD measurements

CD spectra of the amphiphiles were recorded using a JASCO J-815 spectropolarimeter, fitted with a Peltier temperature controller. All

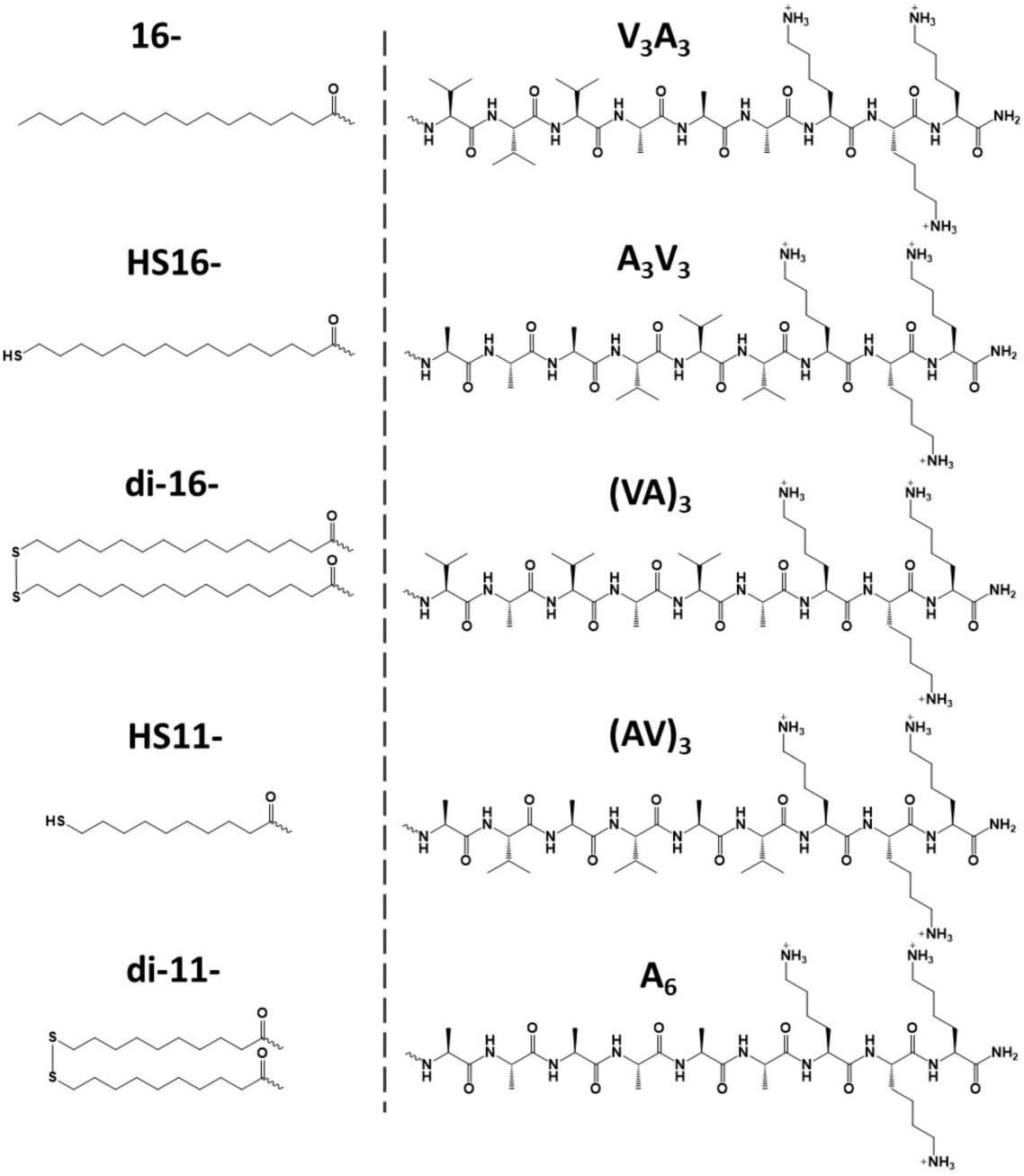

SCHEME 1 Peptide amphiphiles were generated as a combination of one of the alkyl chain options and one of the peptide sequences resulting in 25 different peptide amphiphiles. **Di-16-** and **di-11-** peptide amphiphiles comprised two identical molecules dimerized via the thiols to form a disulfide bond

measurements were performed at 20 °C. Unless stated otherwise, lyophilized powders of peptide amphiphiles were dissolved in 10 mM phosphate buffer (PB), pH 5.8, at the following concentrations: 50 μM for peptide amphiphiles terminated with **16-** and **HS16-** alkyl chains; 25 μM for peptide amphiphiles terminated with **di-16-** chains; 250 μM for peptide amphiphiles terminated with **HS11-** alkyl chains; and 125 μM for peptide amphiphiles terminated with **di-11-** alkyl chains. Samples were left in the dark in sealed vials for 14 days to age before being measured. Spectra were recorded from 260 to 190 nm at 1 nm intervals with a 1 nm bandwidth. All spectra were converted to mean residue ellipticity (deg cm^2 dmol^{-1} res^{-1}) using Equation (1):

$$[\theta] = \frac{100 * [\theta]obs}{c * n * l}, \quad (1)$$

where $[\theta]_{obs}$ is the observed ellipticity in mdeg, c is the concentration of the sample in mM, n is the number of amino acids in the amphiphile and l is the path length of the cuvette in cm.

2.6 | Infrared spectroscopy measurements

ATR-IR spectra were recorded on an Excalibur FTS 4000 setup equipped with a "golden gate." A lyophilized powder of a peptide amphiphile was placed on top of the crystal and a spectrum was recorded (512 scans at 2 cm^{-1} aperture). Deconvolution and fitting of the Amide I peaks to the Lorenz function were performed using Origin Pro.

2.7 | Transmission electron microscopy

For TEM measurements, a 10 μL droplet of the sample (in PB, pH 5.8) was placed on a continuous carbon grid on a copper support (200 mesh) and left for 20 seconds. The excess liquid was removed by manually blotting with filter paper. The grid was washed with deionized water once and blotted again. Uranyl acetate staining (0.5% w/v) was applied, followed immediately by blotting. Images were collected on a JEM1400 Plus (JEOL) transmission electron microscope operating at 80 kV and equipped with a CCD camera.

2.8 | Determination of oxidation of thiolated peptide amphiphiles

Selected peptide amphiphile stocks were prepared as for CD experiments (i.e., in PB buffer) and divided into aliquots which were stored in the dark in sealed vials. At specific time points, the percentage of free thiols in each sample was determined by performing an Ellman's test. The Ellman's test was performed as follows: Ellman's solution was prepared by dissolving Ellman's reagent (5,5′-dithiobis-(2-nitrobenzoic acid), DTNB) in 0.1 M sodium phosphate buffer, pH 8.0 which contained 1 mM EDTA. This was subsequently added to the peptide amphiphile samples and the absorbance of the solution at 412 nm was recorded. The absorbance at day 0 was taken to represent the peptide amphiphiles in a non-oxidized state (i.e., 100% "free" thiols) and the % of free thiols at subsequent time points was calculated relative to this value.

2.9 | Gold nanorod synthesis

Gold nanorods (GNRs) were synthesized in the presence of CTAB in a two-step process commonly described as a seed-mediated approach. 2-3 nm seeds were prepared by mixing the following solutions under intense stirring at room temperature: CTAB (5 mL, 0.20 M), and $HAuCl_4$ (5 mL, 0.50 mM) with ice-cold $NaBH_4$ (0.60 mL, 10 mM). After 2 minutes of vigorous stirring, the solution was left undisturbed at room temperature for 2 hours. For the overgrowth, solutions of $HAuCl_4$ (50 mL, 1.0 mM) and $AgNO_3$ (200 μL, 100 mM) were gently mixed with CTAB (50 mL, 0.20 M) at 25 °C. After 2 minutes of stirring, ascorbic acid (550 μL, 100 mM) was added. The growth solution underwent a color change from dark yellow to colorless due to reduction of gold. Next, 120 μL of the seed solution was added to the growth solution under vigorous stirring at room temperature. After 6 hours the rods were washed with MilliQ twice (2 × 100 mL) by means of centrifugation to remove the CTAB excess.

2.10 | Coating of GNRs with peptide amphiphiles

Coating of the GNRs was performed via a ligand exchange strategy. The PAs were dissolved in DMSO and added to a stirred GNR suspension. The volumes of PA and GNRs were such that the final concentration of DMSO in the solution was 10% (v/v). After 1 hour, the sample was centrifuged, (14 000 rpm, 10 minutes), and the supernatant removed and replaced with water. To remove any remaining free ligand, two extra centrifugation steps were performed.

3 | RESULTS AND DISCUSSION

3.1 | Peptide amphiphile design

The composition of the peptide and alkyl chain segments of the peptide amphiphiles were altered in order to tune the physical and chemical properties to enable the investigation of these effects on self-assembly. For this, five different peptide domains and five alkyl chains (including two dimerized variants) were investigated (Scheme 1). Peptide sequences investigated in this study contained the nonpolar neutral residues valine and alanine in combination with the positively-charged, polar residue lysine. All peptide sequences comprised a C-terminal amide followed by three Lys residues. Three Val and three Ala residues were combined in different ways to yield $\mathbf{V_3A_3}$, $\mathbf{A_3V_3}$, $\mathbf{(VA)_3}$, and $\mathbf{(AV)_3}$. A peptide comprising six Ala residues ($\mathbf{A_6}$), which is likely to form helical structures, was synthesized for comparison.

We employed alkyl chains with a length of either 11 or 16 carbons. The C16 (palmitoyl) chain is widely employed as it is has been demonstrated to result in more stable assemblies in comparison to shorter alkyl chains.[21,28] A thiolated C11 (undecanoyl) chain was also studied; this length is at the lower limit of that required to induce self-assembly.[29,30] Palmitoylated amphiphiles were denoted as **16-** and thiolated amphiphiles were denoted as **HS16-** and **HS11-** (Scheme 1).

Introduction of a thiol may not only influence molecule-surface interactions but also the peptide amphiphile self-assembly process via dimerization. For this reason, disulfide-bonded molecules were also evaluated (**di-16-** and **di-11-** in Scheme 1).

In total, 25 peptide amphiphiles were synthesized and characterized. Initially, their propensities to form ordered secondary structures were studied using CD spectroscopy and ATR-IR spectroscopy. The morphology of the assemblies was visualized with TEM.

3.2 | Peptide amphiphile self-assembly

Formation of supramolecular structures can be affected by environmental factors, including the concentration of the self-assembling

molecules and the composition of the solvent.[31–33] CD spectroscopy is well-suited to screen peptide amphiphile secondary structure,[24,34,35] therefore the optimal concentration of peptide amphiphiles for reliable CD measurements was determined by recording spectra of **16-V_3A_3** and **HS11-V_3A_3** at different concentrations in water (Figure 1A,B). The resulting spectra are typical for β-structured peptides, which possess a minimum around 216 nm.[24,36] For self-assembled peptide amphiphiles, this minimum can be red-shifted (by up to 10 nm) due to a change in the mutual orientation of the peptide backbones.[24] Both peptide amphiphiles showed a minimum between 220 and 224 nm. **16-V_3A_3** showed comparable CD spectra in the range 25 to 100 μM with a significant decrease in the quality of the signal at 10 μM (Figure 1A). Thus, a concentration of 50 μM was chosen for peptide amphiphiles incorporating **16-**, and **HS16-** alkyl chains, and 25 μM for **di-16-** peptide amphiphiles. A higher optimal concentration was expected for the shorter C11 chain. **HS11-V_3A_3** at 1 mM concentration showed a significant difference in the normalized CD intensity compared to lower concentrations, suggesting that the linear dependence on concentration is lost above 0.5 mM (Figure 1B).[21] At 100 μM a low intensity was recorded, therefore a concentration of 250 μM was chosen for all **HS11-** peptide amphiphiles, and 125 μM for **di-11-** peptide amphiphiles.

The effect of ionic strength on secondary structure was subsequently investigated. **16-$(AV)_3$** was dissolved in water or in 10 mM phosphate buffer (PB) at two different pHs: 5.8 and 7.5 (Figure 1C). Significant differences were observed: **16-$(AV)_3$** prepared in water showed a noticeable presence of α-helical structures (minima at 206 nm and 220 nm), and at pH 7.5 the minimum at 223 nm was attributed to β-structures, although a small shoulder at 210 nm was observed. In PB at pH 5.8 the peptide amphiphile was predominantly β-structured, indicated by a single minimum at 221 nm. Interestingly, at pH 7.5 the maximum was red-shifted and broadened, indicating less-ordered structures were formed. Therefore, samples were analyzed in PB at pH 5.8, although it should be noted that published reports on **16-V_3A_3** utilized neutral pH conditions.[37]

Next, the secondary structures and assembly propensities of all 25 peptide amphiphiles were probed with CD spectroscopy, in 10 mM PB, pH 5.8 (Figure 2). It can be observed that only peptide amphiphiles with the **A_6** domain deviated from the typical β-structure.

The minimum position and peak intensity of **HS16-** peptide amphiphiles were compared to their **16-** counterparts to obtain insight in their β-structure-forming ability and the internal organization within the assemblies. Two parameters are important for characterizing and comparing β-structured amphiphile assemblies: the

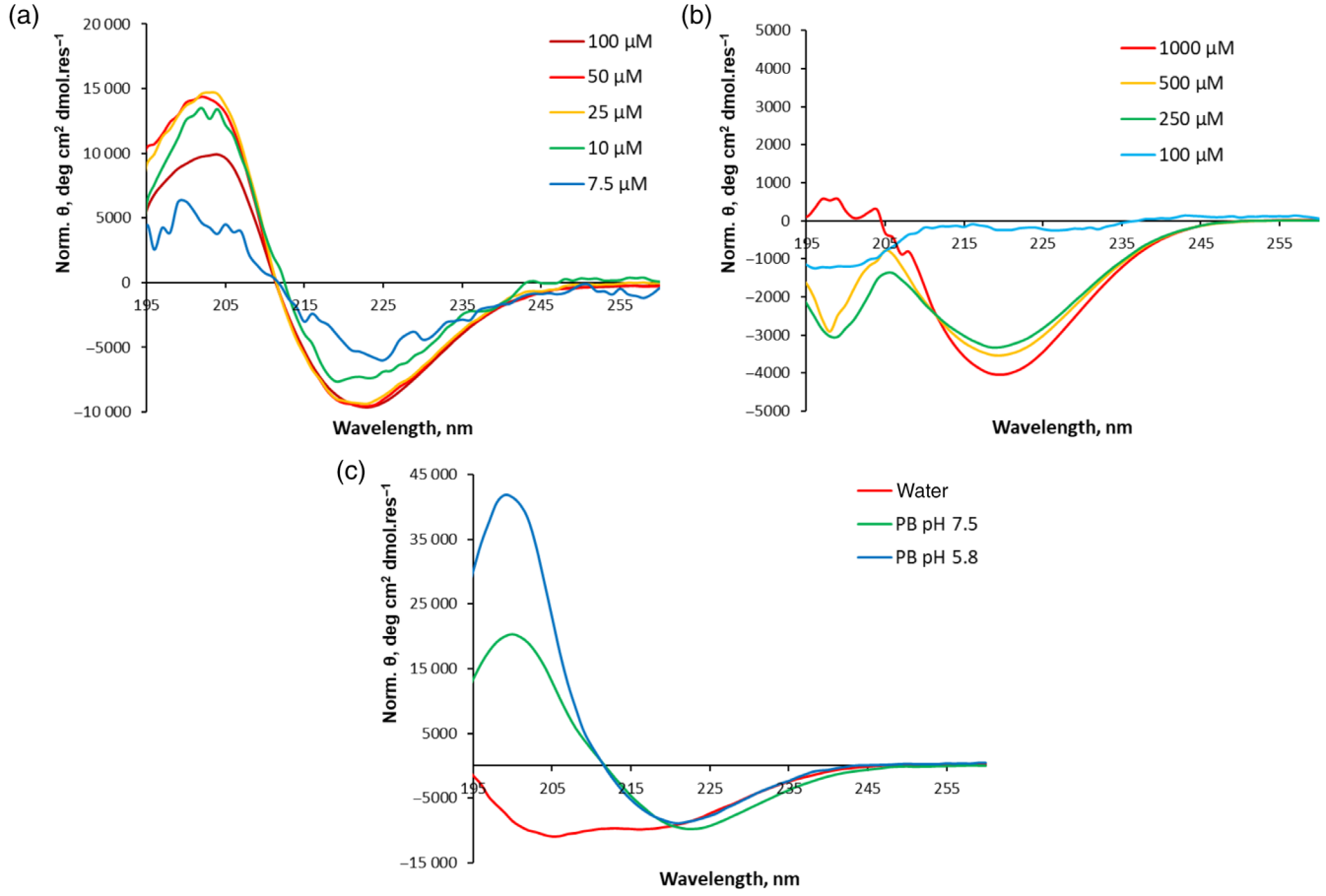

FIGURE 1 Optimization of different conditions for self-assembly monitored with CD spectroscopy: A, **16-V_3A_3** in the concentration range 7.5 to 100 μM (H_2O, no buffer); B, **HS11-V_3A_3** in the concentration range 100 to 1000 μM (H_2O, no buffer); C, **16-$(AV)_3$** prepared in buffer at different pHs, or water. Total [peptide] = 100 μM

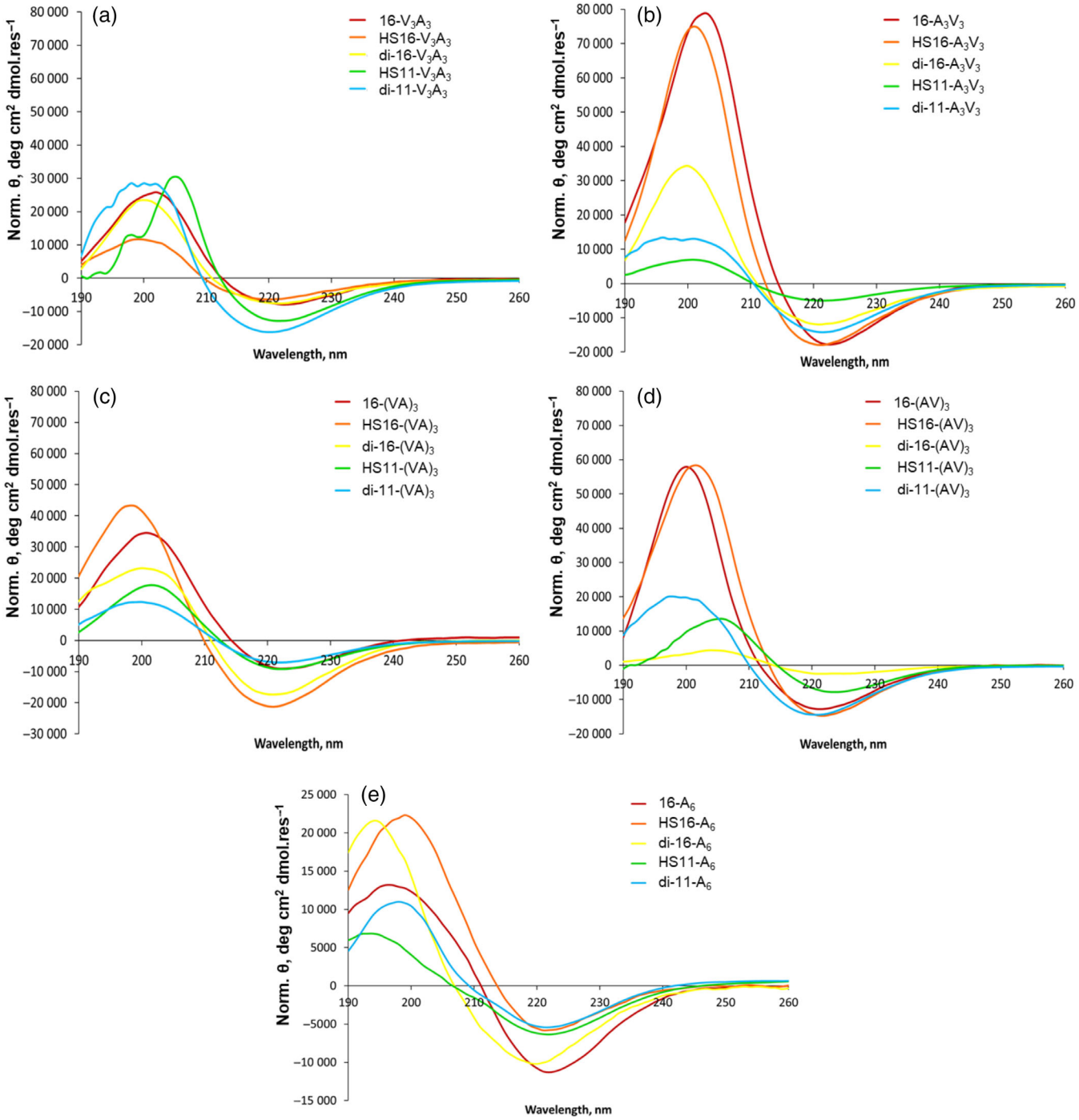

FIGURE 2 CD spectra for peptide amphiphiles: A, **V_3A_3**; B, **A_3V_3**; C, **$(VA)_3$**; D, **$(AV)_3$**; E, **A_6**. Samples were prepared in 10 mM PB (pH 5.8)

position of the ellipticity minimum (θ_{min}) and its intensity.[24] θ_{min} characterizes the orientation of peptide chains within a self-assembled structure. If θ_{min} is located at 216 nm, the peptide chains are likely to be locked into a planar β-strand orientation by means of effective hydrogen bonding alignment. A red-shifted θ_{min} is indicative of less effective hydrogen bond alignment and thus there is more twisting of the peptide chains within the assemblies. Furthermore, the intensity of the spectrum can also provide insights into the assemblies. While self-assembled systems can cause light scattering which affects peak intensities, the differences in the orientations of the β-strands can also affect peak intensities.

While all the **SH16-** and **16-** amphiphiles had minima centered around 221 nm (Figure S26), indicating a shift from the typical position at 216 nm, there were not significant red shifts between the thiolated and non-thiolated C16 variants for any of the peptide sequences studied. Therefore, thiolation of the C16 alkyl chain

does not appear to cause a significant change in the hydrogen bonding of the peptide portion of the amphiphiles within their self-assemblies.

Comparisons between different alkyl chains were more complex to unravel. The $\mathbf{V_3A_3}$ domain did not undergo a significant rearrangement when the **16-** chain was dimerized to form **di-16-**, only a slight blue-shift (~2 nm) in the minimum position was observed (Figures 2A and S26). Shortening the alkyl chain to **HS11-** resulted in a higher molar ellipticity, while dimerization resulted in peak broadening. The reversed sequence, $\mathbf{A_3V_3}$, responded to the alkyl chain alteration differently (Figure 2B): dimerization of **16-** to form **di-16-**$\mathbf{A_3V_3}$ significantly reduced the peak minimum intensity. Shortening the alkyl chain also reduced the peak intensity by almost 25% (Figure S27), but dimerization of **HS11-**$\mathbf{A_3V_3}$ restored the signal to the level of **di-16-**$\mathbf{A_3V_3}$.

Interestingly, thiolation of **16-**$\mathbf{(VA)_3}$ significantly enhanced the intensity of the CD signal, as did dimerization (Figures 2C and S27). No large differences in intensity of the peak minimum were detected for **16-**$\mathbf{(VA)_3}$, **HS11-**$\mathbf{(VA)_3}$, and **di-11-**$\mathbf{(VA)_3}$, yet peak broadening was apparent for the two thiolated amphiphiles. In contrast, $\mathbf{(AV)_3}$ responded to thiolation in a similar fashion as $\mathbf{A_3V_3}$: **di-16-** was less structured than **16-** (Figure 2D). Interestingly, the similarities between the two peptide domains were maintained for the **HS11-** and **di-11-** coupled molecules: the intensity of the **HS11-**$\mathbf{(AV)_3}$ spectrum was significantly lower compared to **di-11-**$\mathbf{(AV)_3}$. This indicates that the peptide domain which is coupled to the alkyl chain affects assembly, and it is possible that the positions of the amino acids within the sequence influence the morphologies of the self-assembly.

$\mathbf{A_6}$ peptide amphiphiles revealed the lowest overall ellipticity signals for all five variants (Figure 2E). Thiolation of the C16 chain led to a significant reduction of the signal, and shortening the thiolated chain to **HS11-**$\mathbf{A_6}$ resulted in a CD spectrum that did not appear to be characteristic for a predominantly β-structured peptide amphiphile. The shoulder which is apparent at 208 nm could be explained by either a blue-shift of the minimum position or a contribution from an α-helical structure.[35] Similar small shoulders were evident for the dimerized molecules **di-16-**$\mathbf{A_6}$ and **di-11-**$\mathbf{A_6}$.

While some similarities and trends between peptide domains could be observed, in particular for the $\mathbf{A_3V_3}$ and $\mathbf{(AV)_3}$ domains, it was clear that both the peptide and alkyl chain domains affected the self-assembly behavior.

To obtain quantitative insights into the β-content within the assemblies, attenuated total reflection Fourier-transform infrared spectroscopy (ATR-FTIR) spectra of lyophilized peptide amphiphiles were recorded (Figures 3 and S28-S32). The Amide I peak is typically centered between 1575-1725 cm^{-1} and represents a superposition of signals derived from different conformations of the peptide backbone: 1627-1640 cm^{-1} is attributed to β-structures; 1647-1654 cm^{-1} to α-structures; and 1650-1670 cm^{-1} to random and other structures.[38,39]

The Amide I peak overlaps with peaks corresponding to the C-terminal amide and the amine of the Lys side chain. Therefore, the Amide I peak was fitted to three peaks with maxima centered around: 1616 cm^{-1} for the C-terminal amide; 1630 cm^{-1} for the amine lysine side-chain, together with β-structures, and; 1669 cm^{-1} for random coil and other structures (Figure 3A). These positions were present in all spectra, although small shifts occurred for some of the samples (Figures S28-S32). If a peak at 1654 cm^{-1}, indicative of α-helix structure, could be resolved, it was added to the fitting procedure. IR spectra of lysine-containing peptides are known to be sensitive to the pH of the solution they are lyophilized from, resulting in a peak shift and peak broadening.[40,41] Although residual TFA was removed, it is possible some traces still remained that affected the position of the observed peaks. Therefore, the joint contribution of β-structures, the C-terminal amide, and primary amines of lysine side chains was compared. This value was considered to reflect the content of β-structures in the samples, while the rest of the Amide I peak was attributed to other structures. The β-associated content for all 25 peptide amphiphiles is summarized in a heatmap (Figure 3B).

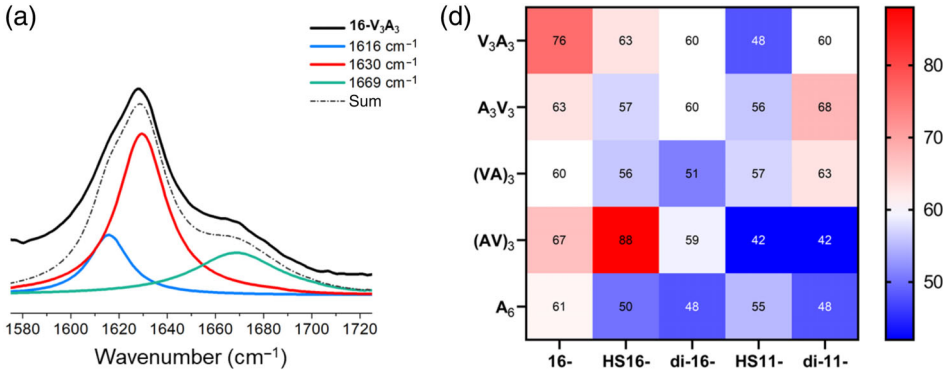

FIGURE 3 Determination of secondary structure content using ATR-IR spectroscopy based on assignment of different contributing secondary structures according to their peaks positions. A, An example of the Amide I peak fitting for **16-**$\mathbf{V_3A_3}$, where the peak centered around 1616 cm^{-1} shows the contribution of the terminal amide (blue line); the peak around 1630 cm^{-1} indicates the presence of β-structures but also the presence of lysine tertiary amines (red line); and the peak around 1667 cm^{-1} is attributed to other structures (cyan line). Relative shifts of the peak maxima were observed for some samples and are likely due to intrinsic factors of self-assembly. B, A heatmap illustrating the β-associated content derived from the Amide I peak fitting; blue shades represent low amounts of β-structure whereas red shades indicate a high percentage of β-structure. Near-white shades indicate an average level of β-structure for these systems. All measurements were performed using freeze-dried, solid samples

It was only possible to resolve a peak at 1654 cm^{-1} for some of the thiolated peptide amphiphiles and it was absent in all palmitoylated peptide amphiphiles (Figures S28-S32). Relatively low levels of β-structure, and therefore of self-assembly, (β-associated content <60% and high α-content—between 10% and 25%), were observed for all **A_6** amphiphiles, with the exception of **16-A_6**, which is in good agreement with the CD data (Figures 2E and S32). For the other peptide amphiphiles, a higher percentage of β-structure was generally observed.

>For the **V_3A_3** peptide domain, 76% β-content was observed with the C16 alkyl chain, although thiolation of this chain resulted in the β-content dropping to 63%. Dimerization of the latter molecule did not significantly change the secondary structure, consistent with the CD spectra. **HS11-V_3A_3** showed only 48% β-content, but **di-11-V_3A_3** was comparable to the C16 peptide amphiphiles. The **A_3V_3** peptide domain showed smaller changes when the alkyl chain composition was altered: the β-associated content varied between 56% and 68% (Figure S28) with **di-11-A_3V_3** being the most β-structured. However, **$(VA)_3$** and **$(AV)_3$** showed more deviant behavior. In general, **16-$(VA)_3$** showed the lowest β-associated content (60%) among all palmitoylated peptide amphiphiles (Figure S30). Although thiolation or shortening the alkyl chain to yield **HS16-** and **HS11-** variants did not significantly change the β-associated content, dimerization of these molecules showed opposing effects with **di-16-$(VA)_3$** showing a decrease in β-structure to 51%, whereas the amount of β-structure in **di-11-$(VA)_3$** increased to 63%. One notable feature was observed for the **$(AV)_3$** peptide domain: it was the only example where thiolation of the C16 chain gave rise to a more β-structured assembly (67% vs 88%, Figure S31). All other variants (**di-16-**, **HS11-**, **di-11-**) showed a β-associated content below 60%.

In some instances, the CD data and the IR analysis appeared to be inconsistent. For example, the CD spectra of **16-$(VA)_3$** and **HS16-$(VA)_3$** would suggest a higher level of self-assembly for the latter, but according to the IR data, the β-associated content did not significantly differ between the two (Figures 2C and 3B). In contrast, **16-$(AV)_3$** and **HS16-$(AV)_3$** had similar CD spectra, however FTIR showed the latter was significantly more β-structured (Figures 2D and 3B). These discrepancies could be attributed to the differences in preparation method: CD spectra were recorded in solution however it was necessary to perform IR experiments with powdered samples, otherwise the signal-to-noise ratio was too high and did not allow for reliable peak fitting. Moreover, we could not prevent some thiol oxidation occurring for both **HS16-** and **HS11-** peptide amphiphiles. We observed oxidation for peptide amphiphiles stored in solution, (Figure S33), and as powders, (Figure S34); however, oxidation occurred faster for the peptide amphiphiles that were in solution. Therefore it is possible that another reason for this discrepancy could be partial oxidation of the thiolated amphiphiles in solution.

It is clear from both the CD and FTIR studies that finding common self-assembly trends, and linking these to secondary structure, is not trivial. In general, thiolated peptide amphiphiles were less structured than their C16 counterparts, although significant (>60%) amounts of β-structure were still observed. However, dimerization, and substitution of the C16 alkyl chain for C11, had different impacts depending on the peptide sequence.

To obtain more insight on the effect of thiolation and dimerization of peptide amphiphiles on self-assembly in solution, TEM was performed.

3.3 | Evaluation of peptide amphiphile fibers using TEM

All peptide amphiphiles assembled into fibers, (Figure 4), as was previously reported for palmitoyl (C16) peptide amphiphiles.[42] This indicated that thiolation did not disrupt self-assembly; thus sequestration of the alkyl chains from the aqueous environment due to effective hydrophobic collapse was maintained. Quantitative information such as true fiber thickness could not be obtained as images were acquired relatively close to focus, with a certain defocus needed, and most of the samples bundled, plus negative staining was performed. Nonetheless, it was determined that all observed fibers had a diameter of ~9 nm, corresponding to the length of two peptide amphiphiles.[43] However, it was evident that there were differences in the fiber appearance for the different samples.

Fibers comprising palmitoyl peptide amphiphiles were long (typically >500 nm) and aligned into sheets (top panels in Figure 4). Fracturing of these fiber stacks appeared to be present in some images, see for example, **16-$(AV)_3$**. Sample preparation could have caused this as samples were blotted and dried on the TEM grid.[44] Moreover, when the top two rows of Figure 4 were compared, it was obvious that thiol introduction reduced the average fiber length irrespective of peptide domain composition. Furthermore, all five dimeric (**di-16-**) peptide amphiphiles also formed short fibers (<200 nm).

In contrast, no general trend was observed for **HS11-** peptide amphiphiles: **HS11-V_3A_3**, **HS11-A_3V_3**, and **HS11-$(VA)_3$** showed a similar length distribution to their **HS16-** counterparts, and bundling was also evident. Intense bundling was observed for **HS11-$(AV)_3$** whereas **HS11-A_6** fibers exhibited no interactions. In addition, no clear tendency was observed that would unify the effect of dimerization for **HS11-** peptide amphiphiles. The appearance of the fibers was altered in every case, with the exception of **di-11-V_3A_3**. For **di-11-A_6** the fibers were longer, appeared to be more defined, and formed bundles. Bundling was also apparent for **di-11-A_3V_3** and **di-11-$(AV)_3$**, whereas for **di-11-$(VA)_3$** the interactions between individual fibers were reduced.

Due to the variety of assemblies, it appeared that the self-assembly of C11 peptide amphiphiles was more sensitive toward the peptide sequence as compared to their C16 variants. In addition, most of the **HS11-** peptide amphiphiles showed less β-associated content and/or significant contributions of α-structures and other structures. However, this is to be expected as it is known that self-assembly of amphiphiles with shorter alkyl chains is less robust.[29,30] In addition, a clear difference between **V_3A_3**, and **$(VA)_3$**, in comparison to **A_3V_3**, **$(AV)_3$**, or **A_6** was observed: the latter amphiphiles tended to form

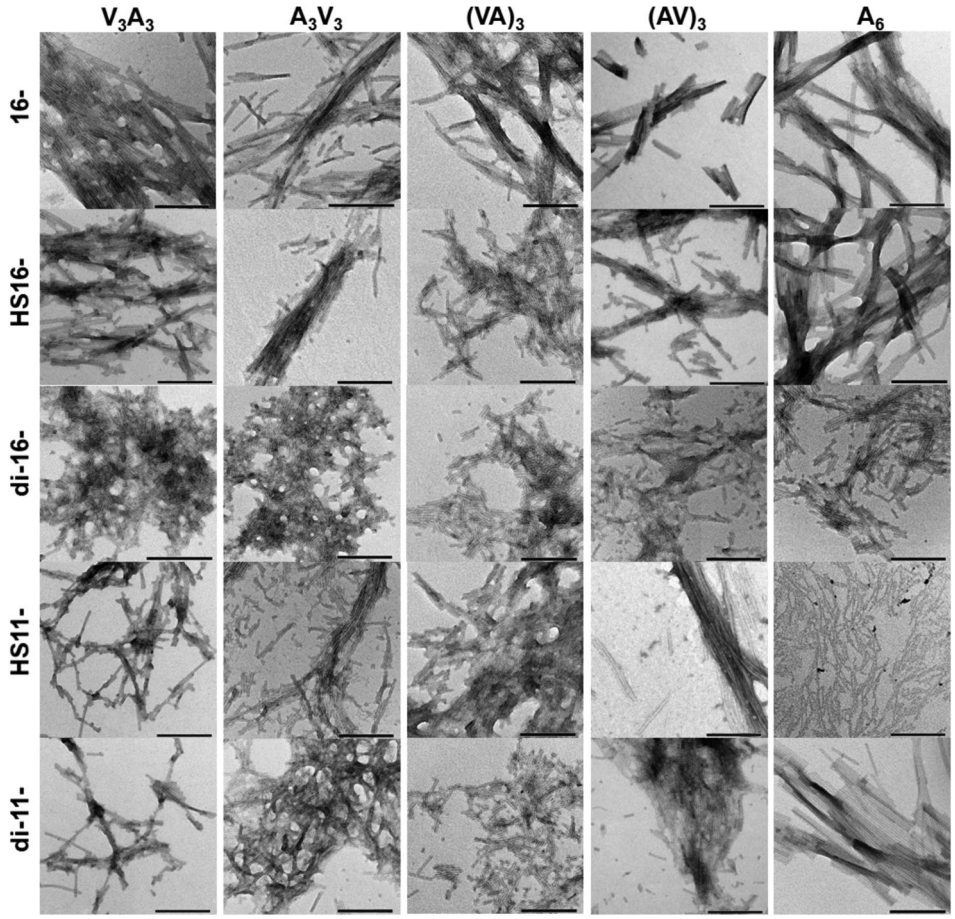

FIGURE 4 Representative TEM images of peptide amphiphiles (uranyl acetate stained). Columns show the same peptide domain conjugated to different alkyl chains, while rows show the same alkyl chain conjugated to different peptides. Samples were prepared in 10 mM PB (pH 5.8) at peptide amphiphile concentrations of: 50 μM for **16-** and **HS16-** samples; 25 μM for **di-16-**; 250 μM for **HS11-**; and 125 μM for **di-11-**. Scale bar is 200 nm

rope-like fiber bundles covering vast areas, while the former amphiphiles yielded smaller-scale structures.

In summary, TEM imaging revealed differences in fiber appearance, in particular for thiolated peptide amphiphiles. Additionally, differences between fibers formed by highly β-structured molecules (such as all **16-** samples) and molecules with high percentages of α-content (e.g., **HS11-A_6** which exhibited 25% α-structures) was observed. Peptide amphiphiles coupled to the **V_3A_3** peptide headgroup were arguably the only group that exhibited relatively similar fiber appearances for all five alkyl chain variants.

3.4 | Implications for self-assembly

It is clear from the CD, FTIR, and TEM data that the secondary structure and morphology of all amphiphiles are affected by changes to the length of, and presence or absence of a thiol on, the alkyl chain attached to the peptide portion. Although, for the CD spectra, the position of the ellipticity minimum is not significantly altered (Figure S26), the intensity of the spectra varies for all the amphiphiles tested (Figure S27). The amount of secondary structure attributed to β-structures, as determined by FTIR, also fluctuates significantly when peptide amphiphiles with identical peptide domains are compared. It is challenging to find trends to these changes in self-assembly; this issue is further complicated by the fact that the CD and FTIR data do not always correlate as the CD spectra were recorded in solution, while FTIR data had to be obtained with solid samples otherwise the signal-to-noise ratio was too high to permit reliable fitting of the data. In addition, some disulfide bond formation occurred with the thiolated amphiphiles, (Figure S33), which is also likely to cause discrepancies. Despite this disulfide bond formation, the data does indicate that there are differences in the secondary structure and fiber morphologies of the thiolated (and partially oxidized), and disulfide-bonded (i.e., fully oxidized), peptide amphiphiles.

One intriguing observation can be made from these data, in combination with the TEM images. It appears that peptide geometry plays a role in self-assembly as we observed that the "block" sequences, **V_3A_3** and **A_3V_3** were less influenced by alterations to the alkyl chain length composition. These peptides consistently demonstrated more-ordered self-assemblies and possessed the ability to adopt a β-strand conformation when coupled to different alkyl chains. In contrast, the alternating sequences **$(VA)_3$** and **$(AV)_3$** were more sensitive to changes

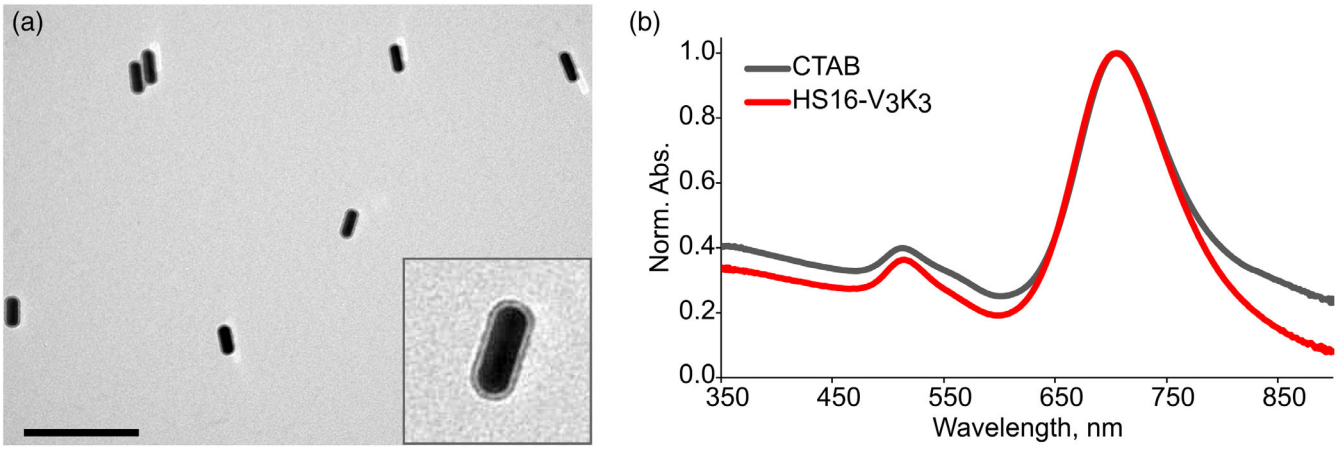

FIGURE 5 Coating of GNRs (44 by 13 nm) with **HS16-V_3A_3**: A, a representative TEM image of the coated GNRs (scale bar = 200 nm), with the inset showing a zoomed image of a single GNR with the peptide amphiphile coating visible, and; B, UV–Vis spectra of GNRs before (**CTAB**, gray line) and after peptide amphiphile coating (**HS16-V_3A_3**, red line)

to the alkyl chain composition. These sequences showed dramatically different self-assembly behavior for palmitoyl and thiolated variants, as well as for monomeric and dimeric species. Such differences in self-assembly have been observed for other constitutionally isomeric peptide amphiphiles, where it was concluded that the side-chain interactions play a significant role in guiding self-assembly.[32] In this study, we expand this concept to include the effects of the alkyl chains and it can clearly be observed that the alkyl chains do indeed influence the self-assembly of the amphiphiles, as well as the type of secondary structures formed.

4 | CONCLUSIONS

We have generated a series of 25 peptide amphiphiles comprising different amino acid sequences and alkyl chain lengths, with some possessing a thiolated alkyl chain terminus. These amphiphiles have been characterized to establish their secondary structure and self-assembly properties in order to determine the factors that affect self-assembly.

Importantly, all the studied amphiphiles possessed a predominant β-sheet secondary structure and self-assembled to form fibers. Although the fibers differed in morphology, it was evident that introduction of a thiol did not prevent assembly into supramolecular structures. If such self-assembly can be translated from solution to a surface, such amphiphiles could prove to be stabilizing coatings for nanoparticles.[45] In particular, the **V_3A_3** peptide domain exhibited high levels of self-assembly and appeared to be most robust in terms of preserving the β-content upon modification of the alkyl chain. Therefore, this peptide domain appears to be the most suited for functionalization of metal surfaces, such as GNPs. Indeed, we have used the **HS16-$V_3A_3K_3$** peptide amphiphile to coat GNRs, and have shown that the GNRs are well-dispersed and that the characteristic plasmon absorption band is not altered by the presence of the peptide amphiphile coating (Figure 5).

CONFLICT OF INTEREST

The authors declare no competing interests.

DATA AVAILABILITY STATEMENT

The data that supports the findings in this manuscript is available from the corresponding author on request.

ORCID

Elena A. Egorova https://orcid.org/0000-0003-4548-5104
Alexander Kros https://orcid.org/0000-0002-3983-3048
Aimee L. Boyle https://orcid.org/0000-0003-4176-6080

REFERENCES

[1] E. C. Dreaden, L. A. Austin, M. A. Mackey, M. A. El-Sayed, *Ther. Deliv.* **2012**, *3*, 457.
[2] L. C. Kennedy, L. R. Bickford, N. A. Lewinski, A. J. Coughlin, Y. Hu, E. S. Day, J. L. West, R. A. Drezek, *Small* **2011**, *7*, 169.
[3] R. S. Riley, E. S. Day, *Wiley Interdiscip. Rev. Nanomed. Nanobiotechnol.* **2017**, *9*, e1449.
[4] P. Zijlstra, P. M. R. Paulo, M. Orrit, *Nat. Nanotechnol.* **2012**, *7*, 379.
[5] P. M. R. Paulo, P. Zijlstra, M. Orrit, E. Garcia-Fernandez, T. C. S. Pace, A. S. Viana, S. M. B. Costa, *Langmuir* **2017**, *33*, 6503.
[6] J. Gao, D. Liu, Z. Wang, *Anal. Chem.* **2008**, *80*, 8822.
[7] C. M. Goodman, C. D. McCusker, T. Yilmaz, V. M. Rotello, *Bioconjugate Chem.* **2004**, *15*, 897.
[8] M. Bhamidipati, L. Fabris, *Bioconjugate Chem.* **2017**, *28*, 449.
[9] N. Bogliotti, B. Oberleitner, A. Di-Cicco, F. Schmidt, J. C. Florent, V. Semetey, *J. Colloid Interf. Sci.* **2011**, *357*, 75.
[10] F. Schulz, W. Friedrich, K. Hoppe, T. Vossmeyer, H. Weller, H. Lange, *Nanoscale* **2016**, *8*, 7296.
[11] K. Fytianos, L. Rodriguez-Lorenzo, M. J. D. Clift, F. Blank, D. Vanhecke, C. von Garnier, A. Petri-Fink, B. Rothen-Rutishauser, *Nanomed. Nanotechnol.* **2015**, *11*, 633.
[12] S. H. Liu, M. Y. Han, *Chem. Asian J.* **2010**, *5*, 36.

[13] C. Hanske, M. N. Sanz-Ortiz, L. M. Liz-Marzan, *Adv. Mater.* **2018**, *30*, e1707003.
[14] B. R. Knowles, D. Yang, P. Wagner, S. Maclaughlin, M. J. Higgins, P. J. Molino, *Langmuir* **2019**, *35*, 1335.
[15] G. I. Sakellari, N. Hondow, P. H. E. Gardiner, *Chemosensors* **2020**, *8*, e80.
[16] A. Gupta, D. F. Moyano, A. Parnsubsakul, A. Papadopoulos, L. S. Wang, R. F. Landis, R. Das, V. M. Rotello, *ACS Appl. Mater. Interfaces.* **2016**, *8*, 14096.
[17] R. Levy, N. T. K. Thanh, R. C. Doty, I. Hussain, R. J. Nichols, D. J. Schiffrin, M. Brust, D. G. Fernig, *J. Am. Chem. Soc.* **2004**, *126*, 10076.
[18] B. C. Mei, E. Oh, K. Susumu, D. Farrell, T. J. Mountziaris, H. Mattoussi, *Langmuir* **2009**, *25*, 10604.
[19] C. P. Shaw, D. A. Middleton, M. Volk, R. Levy, *ACS Nano* **2012**, *6*, 1416.
[20] E. Colangelo, Q. Chen, A. M. Davidson, D. Paramelle, M. B. Sullivan, M. Volk, R. Levy, *Langmuir* **2017**, *33*, 438.
[21] M. P. Hendricks, K. Sato, L. C. Palmer, S. I. Stupp, *Acc. Chem. Res.* **2017**, *50*, 2440.
[22] S. Cavalli, D. C. Popescu, E. E. Tellers, M. R. J. Vos, B. P. Pichon, M. Overhand, H. Rapaport, N. A. J. M. Sommerdijk, A. Kros, *Angew. Chem. Int. Ed.* **2006**, *45*, 739.
[23] S. Cavalli, J. W. Handgraaf, E. E. Tellers, D. C. Popescu, M. Overhand, K. Kjaer, V. Vaiser, N. A. J. M. Sommerdijk, H. Rapaport, A. Kros, *J. Am. Chem. Soc.* **2006**, *128*, 13959.
[24] E. T. Pashuck, H. Cui, S. I. Stupp, *J. Am. Chem. Soc.* **2010**, *132*, 6041.
[25] H. A. Behanna, J. J. J. M. Donners, A. C. Gordon, S. I. Stupp, *J. Am. Chem. Soc.* **2005**, *127*, 1193.
[26] S. E. Paramonov, H. W. Jun, J. D. Hartgerink, *J. Am. Chem. Soc.* **2006**, *128*, 7291.
[27] N. B. Malkar, J. L. Lauer-Fields, D. Juska, G. B. Fields, *Biomacromolecules* **2003**, *4*, 518.
[28] T. J. Moyer, J. A. Finbloom, F. Chen, D. J. Toft, V. L. Cryns, S. I. Stupp, *J. Am. Chem. Soc.* **2014**, *136*, 14746.
[29] I. W. Hamley, *Soft Matter* **2011**, *7*, 4122.
[30] X. D. Xu, Y. Jin, Y. Liu, X. Z. Zhang, R. X. Zhuo, *Colloids Surf., B* **2010**, *81*, 329.
[31] H. Cui, T. Muraoka, A. G. Cheetham, S. I. Stupp, *Nano Lett.* **2009**, *9*, 945.
[32] H. G. Cui, A. G. Cheetham, E. T. Pashuck, S. I. Stupp, *J. Am. Chem. Soc.* **2014**, *136*, 12461.
[33] A. T. Preslar, L. M. Lilley, K. Sato, S. R. Zhang, Z. K. Chia, S. I. Stupp, T. J. Meade, *ACS Appl. Mater. Interfaces* **2017**, *9*, 39890.
[34] S. M. Kelly, N. C. Price, *Biochim. Biophys. Acta* **1997**, *1338*, 161.
[35] N. J. Greenfield, *Nat. Protoc.* **2006**, *1*, 2876.
[36] A. Kawamura, K. Nakanishi, N. Berova, *Methods Enzymol.* **2000**, *312*, 217.
[37] D. S. Ferreira, A. P. Marques, R. L. Reis, H. S. Azevedo, *Biomater. Sci.* **2013**, *1*, 952.
[38] Y. N. Chirgadze, N. A. Nevskaya, *Biopolymers* **1976**, *15*, 627.
[39] H. Susi, D. M. Byler, *Methods Enzymol.* **1986**, *130*, 290.
[40] S. Y. Venyaminov, N. N. Kalnin, *Biopolymers* **1990**, *30*, 1243.
[41] M. Rozenberg, G. Shoham, *Biophys. Chem.* **2007**, *125*, 166.
[42] C. J. Newcomb, S. Sur, J. H. Ortony, O. S. Lee, J. B. Matson, J. Boekhoven, J. M. Yu, G. C. Schatz, S. I. Stupp, *Nat. Commun.* **2014**, *5*, e3321.
[43] F. Tantakitti, J. Boekhoven, X. Wang, R. V. Kazantsev, T. Yu, J. H. Li, E. Zhuang, R. Zandi, J. H. Ortony, C. J. Newcomb, L. C. Palmer, G. S. Shekhawat, M. O. de la Cruz, G. C. Schatz, S. I. Stupp, *Nat. Mater.* **2016**, *15*, 469.
[44] C. J. Newcomb, T. J. Moyer, S. S. Lee, S. I. Stupp, *Curr. Opin. Colloid Interface Sci.* **2012**, *17*, 350.
[45] E. A. Egorova, M. M. J. van Rijt, N. Sommerdijk, G. S. Gooris, J. A. Bouwstra, A. L. Boyle, A. Kros, *ACS Nano* **2020**, *14*, 5874.

SUPPORTING INFORMATION

Additional supporting information may be found online in the Supporting Information section at the end of this article.

How to cite this article: E. A. Egorova, G. S. Gooris, P. Luther, J. A. Bouwstra, A. Kros, A. L. Boyle, *Pept. Sci.* **2021**, *113*(6), e24236. https://doi.org/10.1002/pep2.24236